Delineation of a Carcinogenic *Helicobacter pylori* Proteome*

Aime T. Franco‡, David B. Friedman§, Toni A. Nagy‡, Judith Romero-Gallo‡, Uma Krishna‡, Amy Kendall¶, Dawn A. Israel‡, Nicole Tegtmeyer‖, M. Kay Washington**, and Richard M. Peek, Jr.‡ ‡‡

Helicobacter pylori **is the strongest known risk factor for gastric adenocarcinoma, yet only a fraction of infected persons ever develop cancer. The extensive genetic diversity inherent to this pathogen has precluded comprehensive analyses of constituents that mediate carcinogenesis. We previously reported that *in vivo* adaptation of a non-carcinogenic *H. pylori* strain endowed the output derivative with the ability to induce adenocarcinoma, providing a unique opportunity to identify proteins selectively expressed by an oncogenic *H. pylori* strain. Using a global proteomics DIGE/MS approach, a novel missense mutation of the flagellar protein FlaA was identified that affects structure and function of this virulence-related organelle. Among 25 additional differentially abundant proteins, this approach also identified new proteins previously unassociated with gastric cancer, generating a profile of *H. pylori* proteins to use in vaccine development and for screening persons infected with strains most likely to induce severe disease.** ***Molecular & Cellular Proteomics 8:1947–1958, 2009.***

Helicobacter pylori is a Gram-negative bacterial species that selectively colonizes gastric epithelium and induces an inflammatory response within the stomach that persists for decades (1, 2). Biological costs incurred by the long term relationship between *H. pylori* and humans include an increased risk for distal gastric adenocarcinoma (3–8), and eradication of this pathogen significantly decreases cancer risk among infected individuals without premalignant lesions (9). However, only a fraction of colonized persons ever develop neoplasia, and enhanced cancer risk is related to *H. pylori* strain differences, inflammatory responses governed by host genetic diversity, and/or specific interactions between host and microbial determinants (10).

From the ‡Division of Gastroenterology, Departments of Medicine and Cancer Biology, §Mass Spectrometry Research Center, Department of Biochemistry, and Departments of ¶Biological Sciences and **Pathology, Vanderbilt University School of Medicine, Nashville, Tennessee 37232 and ‖School of Biomolecular and Biomedical Science, University College Dublin, Belfield Campus, Ardmore House, Dublin 4, Ireland

Received, March 13, 2009, and in revised form, May 5, 2009

Published, MCP Papers in Press, May 25, 2009, DOI 10.1074/mcp.M900139-MCP200

H. pylori strains are remarkably diverse (11–15), and the genetic composition of strains can change over time within an individual colonized stomach (16, 17). Despite this diversity, several genetic loci have been identified that augment disease risk. The *cag* pathogenicity island encodes a type IV bacterial secretion system, and the product of the terminal gene in this island, CagA, is translocated into host epithelial cells by the *cag* secretion system following adherence (18–20). Within the host cell, CagA undergoes Src- and Abl-dependent tyrosine phosphorylation (21) and activates the eukaryotic phosphatase SHP-2, leading to dephosphorylation of host cell proteins and cellular morphological changes (19–21). CagA also dysregulates β-catenin signaling (22, 23) and apical-junctional complexes (24), events linked to increased cell motility and oncogenic transformation in several models (25, 26). Another *H. pylori* constituent linked to gastric cancer is the cytotoxin VacA, encoded by the gene *vacA*, which is present in virtually all *H. pylori* strains (27). *In vitro*, VacA induces the formation of intracellular vacuoles (27) and can induce apoptosis (28), and vacuolating activity is significantly associated with the presence of the *cag* pathogenicity island (3).

Approximately 20% of *H. pylori* bind to gastric epithelial cells *in vivo* (29), and sequence analysis has revealed that the *H. pylori* genome contains an unusually high number of ORFs relative to its genome size that are predicted to encode outer membrane proteins (15). BabA, a member of a family of highly conserved outer membrane proteins and encoded by the strain-specific gene *babA2*, binds the Lewis^b histo-blood group antigen on gastric epithelial cells (30, 31), and *H. pylori babA2*$^+$ strains are associated with an increased risk for gastric cancer (30). However, not all persons infected with *cag*$^+$ *babA2*$^+$ toxigenic strains develop gastric cancer, indicating that additional *H. pylori* constituents are important in carcinogenesis.

We recently identified a strain of *H. pylori*, 7.13, that reproducibly induces gastric cancer in two rodent models of gastritis, Mongolian gerbils and hypergastrinemic INS-GAS mice (22). This strain was derived via *in vivo* adaptation of a clinical *H. pylori* strain, B128, which induces inflammation, but not cancer, in rodent gastric mucosa. The oncogenic 7.13 phenotype is not due to an enhanced ability of strain 7.13 to colonize as there were no significant differences in gastric colonization density or efficiency between strains B128 and 7.13 as assessed by either quantitative culture or histology.

However, carcinogenic strain 7.13 binds more avidly to gastric epithelial cells *in vitro* than does strain B128, suggesting that the two strains may variably express different outer membrane proteins.

To define proteins that may mediate the development of *H. pylori*-induced gastric cancer, we performed two-dimensional (2D)[1] DIGE coupled with MS to identify differentially abundant membrane-associated and cytosolic proteins from non-carcinogenic *H. pylori* strain B128 and its carcinogenic derivative, strain 7.13 (22). DIGE/MS is a well established proteomics technology based on conventional 2D gel protein separations whereby prelabeling samples with spectrally resolvable fluorescent dyes and multiplexing samples onto a series of gels that contain a mixture of all experimental samples (internal standard) provide quantitative data on abundance changes for thousands of intact proteins from multiple experimental conditions, each measured in replicate for statistical confidence (32–36). Techniques including DIGE/MS have recently been utilized to robustly define differences in protein abundance profiles between bacterial strains and to compare expression patterns of proteins harvested from bacteria maintained under different growth conditions (37, 38).

Utilizing DIGE/MS, we detected and identified 26 proteins with statistically significant differences between strains B128 and 7.13, including a novel cysteine-to-arginine mutation in the *H. pylori* flagellar protein FlaA. We demonstrate that this FlaA mutation results in structural and functional aberrations. Application of this technique to two genetically related bacterial strains that induce distinct phenotypes also identified several novel candidate *H. pylori* virulence factors, providing a framework for studies targeting the pathogenesis of microbially induced cancer.

EXPERIMENTAL PROCEDURES

Bacterial Strains and Protein Preparation—H. pylori strains B128 and 7.13 were grown in *Brucella* broth with 10% fetal bovine serum (FBS) for 18 h at 37 °C and 5% CO_2 with shaking and harvested by centrifugation at 6,000 × *g* for 10 min as described previously (22). Bacterial pellets were washed once with PBS and then resuspended in PBS with protease inhibitors (Roche Applied Science). To disrupt bacteria, samples were subjected to three rounds of French press-mediated lysis at 20,000 p.s.i. Cellular debris were removed by centrifugation at 5000 × *g* for 10 min. Membrane-associated proteins were collected by ultracentrifugation at 100,000 × *g* for 45 min at 4 °C. The supernatant containing cytosol-associated proteins also was collected for subsequent analysis. The pellet, containing membrane-associated proteins, was resuspended in PBS, subjected to two rounds of rapid freeze-thaw cycles and sonication, and used for subsequent analysis. Levels of total protein in both fractions were quantified by the Bradford assay (Pierce) (17).

DIGE/MS—Quadruplicate samples from each bacterial preparation were independently grown and prepared as described above. For each sample, 0.25 mg of protein was precipitated separately with methanol and chloroform as described previously (39) and resuspended in 30 μl of labeling buffer (7 M urea, 2 M thiourea, 4% CHAPS, 30 mM Tris, 5 mM magnesium acetate). The *N*-hydroxysuccinimide ester dyes Cy2/3/5 were used for minimal labeling using the mixed internal standard methodology of Alban *et al.* (34). For the pH 4–7 experiment, two-thirds (167 μg) of each of the 16 experimental samples (B128 membrane, $n = 4$; B128 cytosol, $n = 4$; 7.13 membrane, $n = 4$; 7.13 cytosol, $n = 4$) were individually labeled with 200 pmol of either Cy3 or Cy5 such that two members of each group were labeled with Cy3 and the other two were labeled with Cy5 to compensate for any dye-specific labeling artifacts. In similar fashion, the remainder of each of the 16 experimental samples (83 μg) were combined and labeled en masse with 800 pmol of Cy2 to generate the mixed internal standard. Labeling was performed for 30 min on ice in the dark after which the reaction was quenched by the addition of 10 mM lysine for 10 min followed by the addition of an equal volume of 2× rehydration buffer (7 M urea, 2 M thiourea, 4% CHAPS, 4 mg/ml DTT). Pairs of Cy3/Cy5-labeled samples were mixed with an equal aliquot of Cy2-labeled mixed internal standard, providing 500 μg of total protein resolved on each gel (Fig. 1). Tripartite labeled samples were brought up to 450 μl with 1× rehydration buffer (7 M urea, 2 M thiourea, 4% CHAPS, 2 mg/ml DTT, 0.5% IPG buffer pH 4–7 or 0.5% IPG buffer pH 7–11). The same procedure was repeated for the pH 7–11 experiment only with 300 μg of total protein on each gel, and quenched samples were brought up to 120 μl in 1× rehydration buffer (with 0.5% IPG buffer pH 7–11) prior to anodic cup loading as described below.

All two-dimensional gel and DIGE-associated instrumentation was manufactured by GE Healthcare. First dimensional separations were performed on a manifold-equipped IPGphor first dimension IEF unit, and second dimensional 12% SDS-PAGE was performed using hand-cast gels for which one plate was presilanized using an Ettan DALT 12 unit according to the manufacturer's protocols. The pH 4–7 samples were passively rehydrated into 24-cm pH 4–7 IPG strips for 24 h prior to IEF, whereas the pH 7–11 samples were applied via anodic cup loading to IPG strips that were rehydrated with DeStreak reagent (GE Healthcare). Cy2/3/5-specific 16-bit data files were acquired at 100-μm resolution separately by dye-specific excitation and emission wavelengths using a Typhoon 9400 Variable Mode Imager, and gels were stained for total protein content with SYPRO Ruby (Molecular Probes/Invitrogen) according to the manufacturer's instructions.

The DeCyder v6.5 suite of software tools (GE Healthcare) was used for DIGE analysis. The normalized volume ratio of each individual protein spot feature from a Cy3- or Cy5-labeled sample was directly quantified relative to the Cy2 signal from the pooled sample internal standard corresponding to the same spot feature. This was performed for all resolved features in a single gel where no gel-to-gel variation exists between the three co-resolved signals. The individual signals from the Cy2 standard were then used to normalize and compare Cy3:Cy2 and Cy5:Cy2 abundance ratios across each eight-gel set, enabling statistical confidence to be associated with each change in abundance or charge-altering post-translational modification using Student's *t* test and ANOVAs. Unsupervised principle component analysis (PCA) and hierarchical clustering (using Euclidean correlation and average linkage) were performed using the DeCyder Extended Data Analysis module.

Proteins of interest were robotically excised and digested into peptides in gel with modified porcine trypsin protease (Trypsin Gold, Promega, Madison, WI), and the resulting peptides were applied to a stainless steel target using an integrated Spot Handling Workstation (GE Healthcare) according to the manufacturer's recommendations. MALDI-TOF MS and data-dependent TOF/TOF tandem MS/MS was

[1] The abbreviations used are: 2D, two-dimensional; PCA, principal component analysis; MOWSE, molecular weight search; FBS, fetal bovine serum; ANOVA, analysis of variance; TCF, T cell factor; LEF, lymphoid enhancer factor; LPS, lipopolysaccharide.

performed on a Voyager 4700 (Applied Biosystems). The resulting peptide mass maps and the associated fragmentation spectra were collectively used to interrogate *H. pylori* sequences (NCBI non-redundant databases) to generate statistically significant candidate identifications using GPS Explorer software (Applied Biosystems) running the MASCOT v1.9 search algorithm (Matrix Science). Database searches were performed allowing for complete carbamidomethylation of cysteine, partial oxidation of methionine residues, and one missed cleavage. Molecular weight search (MOWSE) scores, number of matched ions (and number of unmatched ions), number of matching ions with independent MS/MS matches, percent protein sequence coverage, and correlation of gel region with predicted molecular weight and pI were collectively considered for each protein identification (Table I and supplemental Table 1). In every case reported, the identified *H. pylori* protein was unequivocally matched and distinct from family members/isoforms. Only proteins identifications with MOWSE scores above 77 (threshold for the 95th percentile confidence interval) are reported. Individual ion scores (for MS/MS) above 41 were similarly within the 95th percentile confidence interval, but ion scores below this threshold were still considered for those cases where MOWSE scores were above 77 (Table I and supplemental Table 1).

Cell Culture, Plasmids, and Reagents—AGS human gastric epithelial cells were grown in RPMI 1640 medium (Invitrogen) with 10% FBS (Sigma) and 20 μg/ml gentamicin in 5% CO_2 at 37 °C. Topflash and Fopflash reporter plasmids and TCF were kind gifts from K. Kinzler and B. Vogelstein (Johns Hopkins University). *H. pylori* strains were grown in *Brucella* broth with 5% FBS for 18 h, harvested by centrifugation, and added to gastric cells at a bacteria:cell concentration of 100:1 (22).

DNA Sequencing—*H. pylori* genomic DNA from strains B128 and 7.13 was extracted as described previously (40). *flaA* was amplified from genomic DNA using the primer pair 5′-CACAACACATTTTGGTGAGC-3′ and 5′-GCGTTAGCCCCATACAAAC-3′. A single product was amplified and purified (MinElute PCR purification kit, Qiagen), and sequence determination was performed by the Vanderbilt University DNA sequencing facility with the same primers using BigDye Terminator chemistry and analyzed on an ABI 3730xl DNA Analyzer (GenBank™ accession numbers EU400215 and EU400216). *HP0310* was amplified with primers 5′-ACCAAACTCACCAAAAAGGG-3′ and 5′-CCATCGGTCCAATGAAAAGAAC-3′ and purified as above. Sequencing was performed using the same primer pair and the primer pair 5′-TCAAATACGACCACTCGC-3′ and 5′-GGGCGTGAAATCATTGTG-3′ (GenBank accession numbers EU410066 and EU410067).

Cloning and Genetic Exchange of flaA Genes between H. pylori Strains B128 and 7.13—To generate the *flaA*-complemented strain, *flaA* with its own promotor was amplified by PCR from strain 7.13 ($flaA^{7.13}$) and cloned into pGEM-Teasy (Promega). A chloramphenicol resistance cassette was inserted within the *flaA* gene to create a suicide knock-out vector as described previously (18). This vector was then used to generate an *flaA* knock-out mutant in strain B128. The successful integration of the chloramphenicol cassette into the $flaA^{B128}$ gene was confirmed by PCR, and the absence of FlaA expression was demonstrated by Western blotting using flagellin-specific rabbit antibodies (data not shown). To transfer the intact $flaA^{7.13}$ gene into the B128 isogenic *flaA* mutant, $flaA^{7.13}$ was fused with another selectable marker, the kanamycin resistance *aphA3* cassette (41). The intergenic region between open reading frames *HP0999* and *HP1000* in the *H. pylori* chromosome was selected as the integration site for complementation of $flaA^{7.13}$. This region is in one of two plasticity zones and has no known function in *H. pylori* colonization or virulence. Specifically the $flaA^{7.13}$-*aphA3* construct was cloned into pBluescript containing the *H. pylori* genes *HP0998-1001*, and this construct was then used to transform the B128 *flaA* isogenic mutant using natural transformation as described previously (41). Double resistant clones were selected on agar plates containing both kanamycin and chloramphenicol, and re-expression of $flaA^{7.13}$ in the B128 isogenic *flaA* mutant was confirmed by Western blotting using flagellin-specific rabbit antibodies (data not shown).

Motility Assays—Soft agar motility assays for *H. pylori* were performed on medium containing *Brucella* broth, 0.35% agar, and 10% (v/v) FBS. A stab of *H. pylori* was spotted into soft agar plates and allowed to incubate for 3–5 days under microaerophilic conditions. Motility was assessed by measuring the diameter of outward migration as swarm halos apparent in the soft agar.

Transmission Electron Microscopy—All *H. pylori* samples for transmission electron microscopy were grown for 24 h on tryptic soy agar plates under microaerobic conditions. *H. pylori* were transferred to carbon-coated copper grids (Electron Microscopy Sciences) by placing grids directly onto plates for 30 s. Samples were fixed with 1% glutaraldehyde for 1 min, rinsed, and negatively stained with 0.05% uranyl formate and 1% uranyl acetate. Samples were visualized and photographed using a Philips CM12 transmission electron microscope (Vanderbilt Cell Imaging Core) operating at 80 keV.

Western Analysis—Isogenic *HP0310*, *HP0391*, *HP0743*, and *HP1286* null mutants were constructed within strain 7.13 by insertional mutagenesis using *aphA* and were selected with kanamycin (25 μg/ml) (22). *H. pylori* were added to AGS cells at a bacteria:cell ratio of 100:1, gastric cell lysates were harvested, and protein concentrations were quantified by the Bradford assay (Pierce). Proteins (20 μg) were separated by SDS-PAGE and transferred to PVDF membranes (Pall Corp.). Levels of intracellular phosphorylated CagA were determined using an anti-pY99 antibody (1:300; Santa Cruz Biotechnology), and actin levels were determined using an anti-actin (C-11) antibody (1:500; Santa Cruz Biotechnology). Primary antibodies were detected using goat anti-rabbit (1:20,000; Sigma) or donkey anti-goat (1:5000; Sigma) horseradish peroxidase-conjugated secondary antibodies, visualized by the ECL detection system (Cell Signaling Technology), and quantified using the ChemiGenius system (Syngene). Densitometric analysis of multiple Western blots was then performed as described previously (22).

Transfections and Luciferase Assays—AGS cells (2×10^5) were transfected with 3 μl of Lipofectamine 2000 (Invitrogen), 1 μg/ml Topflash or 1 μg/ml Fopflash, 0.5 μg/ml TCF/LEF, and 0.5 μg/ml *Renilla* luciferase reporter in Opti-MEM I (Invitrogen) for 5 h. Transfection mixtures were then replaced with complete medium containing *H. pylori* or medium alone. After 24 h, cells were harvested in 1× Passive Lysis Buffer (Promega). Luciferase activity was determined using a luminometer and was normalized to *Renilla* luciferase activity using a Dual-Luciferase reporter assay system (Promega).

Immunofluorescence—Gastric epithelial cells were cultured on glass cover slides, and cells treated with or without *H. pylori* were washed twice with PBS, permeabilized, and fixed with ice-cold methanol at −20 °C as described previously (22). Slides were incubated in 3% BSA (Sigma) for 10 min and then incubated with rabbit anti-β-catenin antibody (1:100; Sigma) overnight at 4 °C. Washed slides were then incubated with goat anti-rabbit IgG-Cy2 (1:100; Molecular Probes) at room temperature for 30 min. For each sample, at least 100 cells were evaluated by an independent observer unaware of experimental conditions.

Animals and H. pylori Challenge—All procedures were approved by the Institutional Animal Care Committee of Vanderbilt University. Male Mongolian gerbils (Harlan, Indianapolis, IN) 4–8 weeks of age were orogastrically challenged with sterile *Brucella* broth or *H. pylori* strains 7.13, an isogenic B128 $flaA^-$ mutant, or an isogenic B128 $flaA^-$ mutant complemented with *flaA* from strain 7.13 and were sacrificed 12–14 weeks postinoculation. One half of the glandular stomach was fixed for histologic examination, and the other half was homogenized

in sterile PBS, plated on selective Trypticase soy agar plates, and incubated for 3–5 days for *H. pylori* culture (22). Linear strips extending from the squamocolumnar junction through proximal duodenum were fixed in 10% neutral buffered formalin. Tissues were paraffin-embedded and stained with hematoxylin and eosin, and indices of inflammation and injury were scored on a 0–3 scale by a single pathologist blinded to treatment groups. Dysplasia/carcinoma were diagnosed using morphologic criteria previously established for gastrointestinal neoplasia in rodent models of disease (22).

Statistical Analysis—Gerbils were considered to be successfully infected if results from histological examination of tissue or culture were positive. ANOVA and Student's *t* tests were used for statistical analyses of intergroup comparisons. Significance was defined as $p < 0.05$.

RESULTS

H. pylori Strains 7.13 and B128 Exhibit Distinct Protein Expression Profiles—We previously demonstrated that *in vivo* adapted *H. pylori* strain 7.13 reproducibly induces premalignant and malignant gastric lesions in two different rodent models, whereas cancer was not induced by the progenitor strain B128 (22). An initial study using DNA array technology failed to detect any significant differences between the strains (data not shown). This result may be based on the fact that differences are post-translational in nature or that point mutations, gene inversions, or small deletions are difficult to detect with this technology. In addition, *H. pylori* DNA arrays are based on sequences derived from two unrelated strains (26695 and J99) and do not contain ORFs that may be unique to strain B128 and/or 7.13. Therefore, we focused on identification of proteomic differences between these two genetically related strains by performing two-dimensional DIGE/MS. To increase the depth of analysis, we first fractionated minimally passaged whole cell bacterial lysates into membrane and cytoplasmic fractions and then analyzed these proteins independently by DIGE with isoelectric points in the pH 4–7 and pH 7–11 range.

Cytoplasmic and membrane fractions were prepared from each strain independently in quadruplicate, and the 16 resulting extracts were co-resolved across eight DIGE gels coordinated by a Cy2-labeled 16-mixture pooled sample internal standard as described under "Experimental Procedures" (Fig. 1). For the pH 4–7 gels, a total of 842 resolved protein features, including many isoforms that result from charged post-translational modification and/or processing, were matched across all eight gels (Fig. 2*A*). Within each gel, direct measurements of expression levels for each resolved protein were obtained between Cy3 and Cy5 channels relative to the Cy2 channel independently without the interference of technical variation because the tripartite labeled proteins co-migrate. This methodology enabled normalization of the Cy3/Cy2 and Cy5/Cy2 intragel ratios between gels by virtue of the signal from the Cy2 internal standard, which was present in each gel. This analysis was performed independently for each of the 842 resolved features.

We anticipated that the greatest source of variation among the four sample categories would be between cytoplasmic and membrane fractions with smaller variations resulting from differences between strains. PCA was used to assess the major sources of variation between samples and to distinguish biologically relevant changes from technical artifacts that may have resulted from either sample preparation, gel

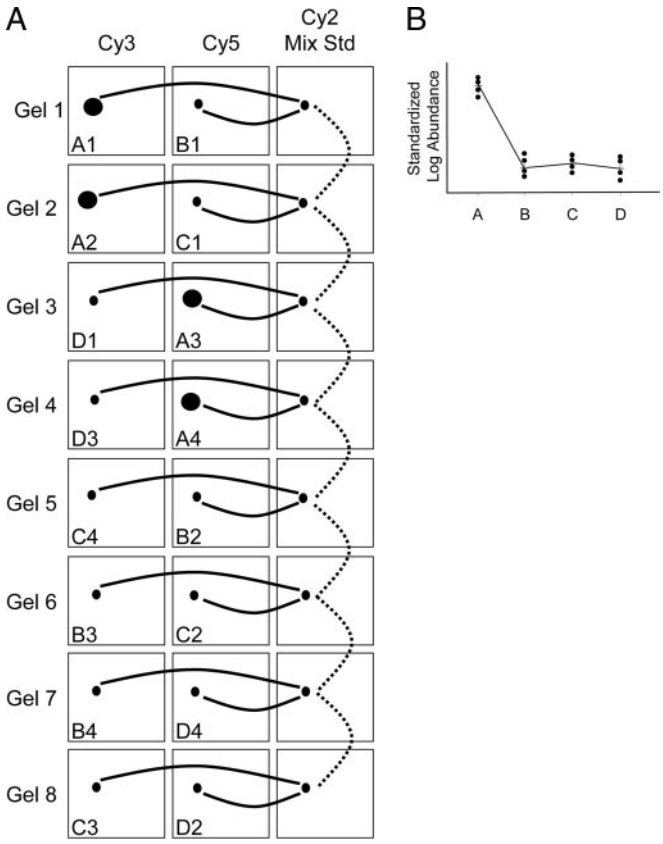

FIG. 1. **DIGE experimental design.** Shown is a schematic of the sample loading matrix within an eight-gel DIGE experiment whereby each gel is coordinated by a Cy2-labeled pooled sample mixture to provide an internal standard for every resolved protein form on each gel. Four classes of samples were co-analyzed (*A*, membrane B128; *B*, membrane 7.13; *C*, cytoplasmic B128; *D*, cytoplasmic 7.13), and samples were prepared independently in quadruplicate. For each class, two of the individual samples were labeled with Cy3 and the other two were labeled with Cy5 to balance any dye-specific labeling artifacts without adding technical replicates into the analysis (which would happen if the same sample were labeled once with each dye). *A*, this eight-gel matrix was used for both pH 4–7 (0.5 mg of total protein) and pH 7–11 (0.3 mg of total protein) isoelectric focusing gradients, producing 16 total DIGE gels. The three dye labelings for a given DIGE gel are grouped *horizontally*. Within the *boxed* regions representing each labeled sample is depicted a theoretical protein that is up-regulated in class A (membrane B128). *Solid lines* illustrate the two independent quantitative ratios made within each gel relative to the cognate signal from the Cy2-labeled internal standard (*Cy2 Mix Std*) without interference from technical variation because the samples are co-resolved within the same gel. The *dotted lines* indicate how these Cy3:Cy2 and Cy5:Cy2 intragel ratios are then normalized between the eight gels. *B*, a graphical representation of the normalized abundance ratios for this theoretical protein change.

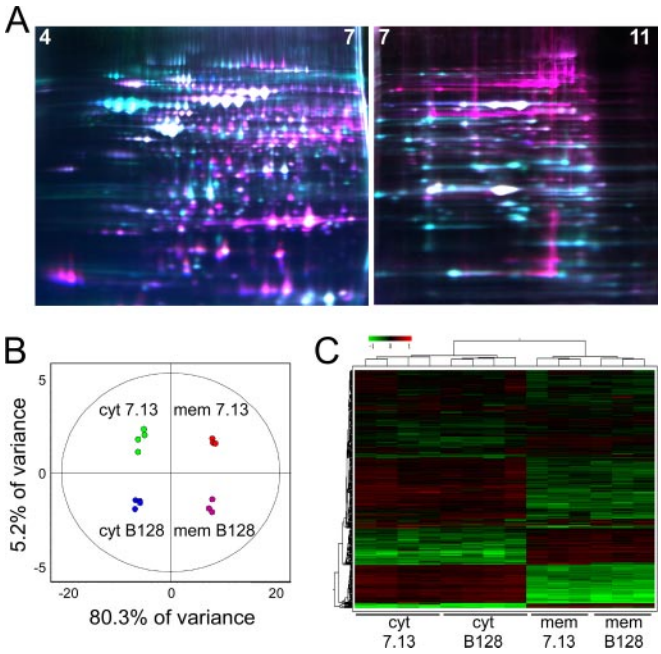

FIG. 2. **Proteome analysis of two *H. pylori* strains using 2D DIGE.** *A*, false colored representative pH 4–7 and pH 7–11 gels contained three differentially labeled samples as described under "Experimental Procedures." Cy2-labeled internal standard (*blue*), Cy3-labeled experimental samples (*green*), and Cy5-labeled experimental samples (*red*) are overlaid in representative gels. *B*, unsupervised PCA accurately segregates the 16 individual DIGE expression maps by two principle components and demonstrates high reproducibility between replicate samples within each group. Values within the *circles* of the PCA plots are within the 95th percentile confidence interval. *C*, unsupervised hierarchical clustering of the 16 individual DIGE expression maps and of individual proteins with relative expression values for each are displayed as a heat diagram using a relative scale from −0.5 (*green*) to +0.5 (*red*). *cyt*, cytoplasm; *mem*, membrane.

electrophoresis, or image acquisition. PCA reduces the complexity of the multidimensional space into two principle components, PC1 and PC2, which orthogonally divide the samples based upon the two largest sources of variation in the data set (Fig. 2*B*).

The protein expression characteristics from all 842 features from each individual sample are represented by each of the 16 data points in the PCA plot (Fig. 2*B*). This analysis demonstrated that 80.3% of the variance (PC1) separated cytoplasmic from membrane samples as expected. An additional 5.2% of variance (PC2) separated the carcinogenic strain 7.13 from the non-carcinogenic strain B128. Similar results were obtained for an additional 300 protein features resolved in the pH 7–11 range (data not shown; PC1 = 84.5%, membrane *versus* cytoplasmic; PC2 = 5%, strain 7.13 *versus* strain B128).

These results were confirmed using unsupervised hierarchical clustering analysis of the 16 independent 842-member proteome maps whereby samples were clustered based on similarities between global expression patterns (represented as an expression matrix heat diagram; Fig. 2*C*). These unbiased analyses demonstrated reproducibility between independent replicate samples and an extremely low level of technical variation and highlighted a discrete subset of protein expression changes representing candidate proteins potentially involved in carcinogenesis.

We next proceeded to identify the subset of proteins that were differentially expressed between the two strains using the univariate Student's *t* test and ANOVAs ($p \leq 0.05$ with many <0.01; Table I and supplemental Table 1). Twenty proteins (often present as multiple charged isoforms) were identified from the pH 4–7 separations as being present at significantly higher or lower levels in carcinogenic strain 7.13 compared with the parental derivative B128 strain (Table I, supplemental Tables 1 and 2, and supplemental Figs. 1 and 2). An additional six proteins were identified from the pH 7–11 separations (Table I, supplemental Tables 1 and 2, and supplemental Figs. 1 and 2). More proteins were observed as decreased *versus* increased in abundance in the carcinogenic *versus* the non-carcinogenic strain.

A C296R Mutation in the FlaA Protein Identified by Proteomics Analysis Results in Altered Bacterial Motility and Morphology—Identification of differentially regulated proteins in a carcinogenic *H. pylori* strain provides a foundation for targeted and rational investigations into the role of specific bacterial factors in virulence. Of particular interest in this regard were apparent changes in levels of the *H. pylori* flagellar protein FlaA (Fig. 3*A*), which is required for a phenotype (motility) implicated in pathogenesis. A detailed analysis indicated that FlaA levels did not differ between strains B128 and 7.13 but that each strain expressed a different series of four FlaA charged isoforms with the two series being slightly offset in pI (Fig. 3*B*). This pI shift for a specific series of FlaA charged isoforms is consistent with a new charged modification that is present on all isoforms or a missense mutation involving a charged amino acid. Because FlaA was found to resolve as at least four distinct charged isoforms, it is likely that this alteration would have been missed using conventional 2D gel analysis where the pI shift for this series of isoforms could easily be mistaken for gel-to-gel variation.

The source of this difference was investigated using MALDI-TOF MS and TOF/TOF tandem MS on gel-resolved FlaA isoforms that were run on separate gels (because the DIGE gels each contained a mixture of samples from both strains). Peptide mass mapping of the resulting in-gel digestion with trypsin protease clearly demonstrated a unique peptide ion at *m/z* 732.38 that was specific to FlaA from strain B128 (Fig. 4, *A* and *B*). The fragmentation pattern that resulted from tandem TOF/TOF MS on this peptide was consistent with the sequence GC^{296}LNLR (Fig. 4*C*). Direct genomic sequencing of *flaA* in both strains confirmed the presence of a single T→C nucleotide substitution that specified a cysteine in strain B128 and an arginine in strain 7.13 at position 296 of the coding sequence (Fig. 5*A*).

TABLE I

Proteins identified as present in differing amounts in membrane and cytosolic fractions of strains 7.13 and B128

Gel position number[a]	NCBI accession number	Gene number[b]	Name	Protein	-Fold difference	*p* value
Membrane fraction: proteins lower in 7.13 *vs.* B128						
21	gi|15644938	HP0310[c]	Hypothetical ORF	Putative protein	−1.87	0.0078
14 (15)	gi|15645139	HP0512	*glnA*	Glutamine synthetase	−1.62	0.043
31	gi|25808199	HP0545	*cag24/cagD*	*cag* pathogenicity island protein	−1.3	0.039
11	gi|7994574	HP0658	*gatB*	Aspartyl/glutamyl-tRNA amidotransferase	−3.58	0.034
18 (17)	gi|15345313	HP0690	*fadA*	Acetyl-CoA acetyltransferase	−1.69	0.031
38 (37, 39, 40)	gi|84626117	HP0875	*katA*	Catalase	−4.04	0.00053
29	gi|4155406	HP0900	*hypB*	Urease nickel incorporation protein	−1.54	0.044
27	gi|15645574	HP0958	Hypothetical ORF	Putative	−2.93	0.0023
16	gi|15645793	HP1179	*deoB*	Phosphopentomutase	−1.58	0.02
44	gi|15645899	HP1286	Hypothetical ORF	Conserved hypothetical secreted protein	−2.02	0.012
1 (2)	gi|15646062	HP1453	Hypothetical ORF	Putative outer membrane protein	−5.95	0.0021
42	gi|15646171	HP1564	Outer membrane protein	Outer membrane protein	−2.2	0.00059
36	gi|4155432	JHP0870	Hypothetical ORF	Hypothetical outer membrane protein	−2.86	0.0014
Membrane fraction: proteins higher in 7.13 *vs.* B128						
22	gi|15644938	HP0310[c]	Hypothetical ORF	Putative protein	3.2	0.02
28	gi|15644959	HP0331	*minD*	Cell division inhibitor	1.33	0.0013
20	gi|2920363	HP0743	*mreB*	Rod shape-determining protein	1.27	0.041
26	gi|15645444	HP0825	*trxB*	Thioredoxin reductase	3.63	0.023
9	gi|18075724	HP1134	*atpA*	ATP synthase α chain	1.65	0.019
Cytosolic fraction: proteins lower in 7.13 *vs.* B128						
30	gi|4154609	HP0110	*grpE*	Co-chaperone and heat shock protein	−1.24	0.0095
35	gi|7188722	HP0243	*napA*	Neutrophil-activating protein	−1.33	0.0091
21	gi|15644938	HP0310[c]	Hypothetical ORF	Putative; homology to polysaccharide deacetylase	−2	0.00017
33	gi|15645018	HP0390	*tagD*	Adhesin-thiol peroxidase	−1.22	0.024
32	gi|15645019	HP0391	*cheW*	Chemotaxis protein	−1.24	0.02
14 (15)	gi|15645139	HP0512	*glnA*	Glutamine synthetase	−1.49	0.0014
31	gi|25808199	HP0545	*cag24/cagD*	*cag* pathogenicity island protein	−1.37	0.014
18 (17)	gi|15345313	HP0690	*fadA*	Acetyl-CoA acetyltransferase	−1.26	0.023
24	gi|15645444	HP0825	*trxB*	Thioredoxin reductase	−1.66	0.0005
38 (37, 39, 40)	gi|84626117	HP0875	*katA*	Catalase	−2.32	0.0038
29	gi|4155406	HP0900	*hypB*	Urease nickel incorporation protein	−1.73	0.00024
27	gi|15645574	HP0958	Hypothetical ORF	Putative protein	−4.76	1.10*e*−07
16	gi|15645793	HP1179	*deoB*	Phosphopentomutase	−1.31	0.043
44	gi|15645899	HP1286	Hypothetical ORF	Conserved hypothetical secreted protein	−1.59	0.0052
42	gi|15646171	HP1564	Outer membrane protein	Outer membrane protein	−1.45	0.0024
23	gi|4155056	JHP0504	*accA*	Acetyl-CoA carboxylase subunit A	−2.94	0.0078
Cytosolic fraction: proteins higher in 7.13 *vs.* B128						
41	gi|15644859	HP0231	Hypothetical ORF	Putative protein	1.29	0.0015
22	gi|15644938	HP0310[c]	Hypothetical ORF	Putative protein	18.8	1.60*e*−07
28	gi|15644959	HP0331	*minD*	Cell division inhibitor	1.25	0.047
43	gi|15645898	HP1285	*hppA*	Acid phosphatase	1.35	0.00039
19	gi|4154912	JHP0387	*pepQ*	Putative proline peptidase	1.32	0.018

[a] Corresponds to gel position number in supplemental Table 1 and supplemental Fig. 1. Gel position numbers in parentheses indicate redundant excisions from charged isoforms that exhibited the same expression pattern.

[b] Corresponds with gene number from the sequenced genome of *H. pylori* 26695 (HP number) or J99 (JHP number).

[c] The apparent abundance change in HP0310 was subsequently determined to be due to differences in isoforms between strains (see text).

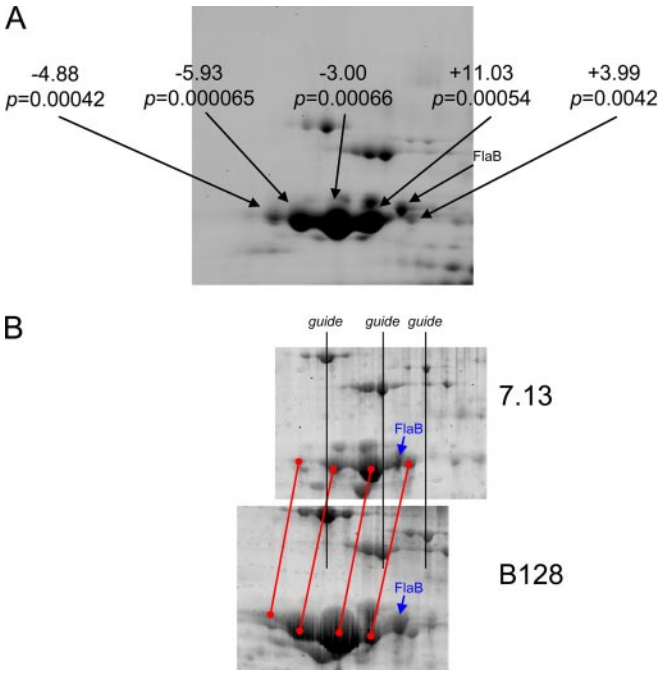

FIG. 3. **Expression of FlaA isoforms in membrane fractions from strains 7.13 *versus* B128 ($n = 4$).** *A*, SYPRO Ruby poststain of one of the eight DIGE gels with relative DIGE expression levels indicated along with the associated *p* value (Student's *t* test) for each FlaA isoform. *B*, 7.13 and B128 samples were resolved on independent gels to enable MS analysis on the two forms separately. *Black guide lines* are shown to reflect proper registration of the two spot patterns including four major FlaA charged isoforms (registered with *red lines*). The position of FlaB, confirmed by MS analysis (supplemental Figs. 1 and 2 and supplemental Table 1), is shown in both panels for reference.

Strains B128 and 7.13 Exhibit Differences in Motility and Ultrastructure—The C296R FlaA amino acid substitution identified by DIGE/MS localized to a predicted helical region. Because differences in flagellar structure can alter motility and motility is essential for colonization and persistence of *H. pylori* (42, 43), we next determined whether differences in motility were present between the two strains. Samples of both *H. pylori* strains were spotted onto soft agar plates and incubated for 3 days, and the resulting diameters of swarm halos were quantified. Strain 7.13 consistently migrated farther and produced larger swarm halos compared with strain B128 (Fig. 5*B*). Thus, data generated from a comparison of these bacterial proteomes directly led to the identification of a specific difference in phenotype in that strain 7.13 is more motile than strain B128 potentially because of differences in flagellar structure.

To further investigate the ramifications of this difference in FlaA sequence, we examined bacterial morphology at the ultrastructural level for both strains using transmission electron microscopy. In strain B128, flagella were frequently closely adjacent and adherent to each other when compared with flagella from strain 7.13. Closely associated flagella were observed in 63% of B128 organisms compared with 22% of 7.13 organisms (Fig. 5*C*). In addition to morphological differences in flagella, the longitudinal body length of strain B128 (2.28 ± 0.12 μm) was significantly greater than that of carcinogenic strain 7.13 (1.82 ± 0.12 μm; Fig. 5*C*), whereas transverse body widths were virtually identical (0.69 *versus* 0.67 μm, respectively). Although the flagella of the two strains appeared equal in length when measured independently, when assessed relative to body length, the flagella of strain 7.13 were approximately twice as long. These results suggest that reduced motility observed in strain B128 may be related to an increase in flagellar adhesiveness conferred by substitution of a cysteine for an arginine at position 296 within FlaA.

To directly test the influence of this FlaA mutation on motility, we complemented an isogenic *flaA*$^-$ knock-out mutant of *H. pylori* strain B128 with the *flaA* allele from carcinogenic strain 7.13 that was integrated at an ectopic site (see "Experimental Procedures"). Re-expression of FlaA from cancer strain 7.13 in a *flaA*$^-$ null B128 background completely restored motility in soft agar (Fig. 6*A*) but only to levels seen with parental strain B128, suggesting that additional factors mediate the increased motility phenotype observed in cancer strain 7.13. We next examined the ability of these mutants to alter CagA translocation and β-catenin activation, phenotypes previously shown to differ between strains B128 and 7.13 (22). In contrast to motility, there were no differences in CagA translocation or β-catenin activation when either of the mutant *flaA* strains were compared with the wild-type strain (data not shown).

Complementation of FlaA from H. pylori Strain 7.13 into Strain B128 per se Does Not Reconstitute an Oncogenic Phenotype in Vivo—We next sought to define the role of FlaA in a model of *H. pylori*-induced carcinogenesis by infecting Mongolian gerbils with *Brucella* broth alone ($n = 10$), strain 7.13 ($n = 10$), an isogenic *flaA*$^-$ B128 mutant ($n = 10$), or the complemented B128 *flaA*$^-$ mutant ($n = 10$). Gerbils were challenged with *H. pylori* and sacrificed 12–14 weeks postinoculation. There was no evidence of gastric inflammation or injury in uninfected control animals. The majority of gerbils (90%) challenged with strain 7.13 were successfully infected and developed acute and chronic gastric inflammation as well as dysplasia as described previously (22). As expected, inactivation of *flaA* in strain B128 led to an inability of this mutant to colonize gerbils, which is consistent with previous reports demonstrating that disruption of flagella abrogates the ability of *H. pylori* to colonize animals (44). Of interest, complementation of *flaA* from strain 7.13 into the isogenic *flaA*$^-$ mutant B128 strain did not restore the ability to colonize gerbils or induce injury. These results indicate that complementation of FlaA from strain 7.13 into strain B128 alone is not sufficient to induce lesions with premalignant potential within the gastric niche.

Additional Proteins Differentially Abundant in Strains B128 and 7.13—In light of the above results, we next sought to

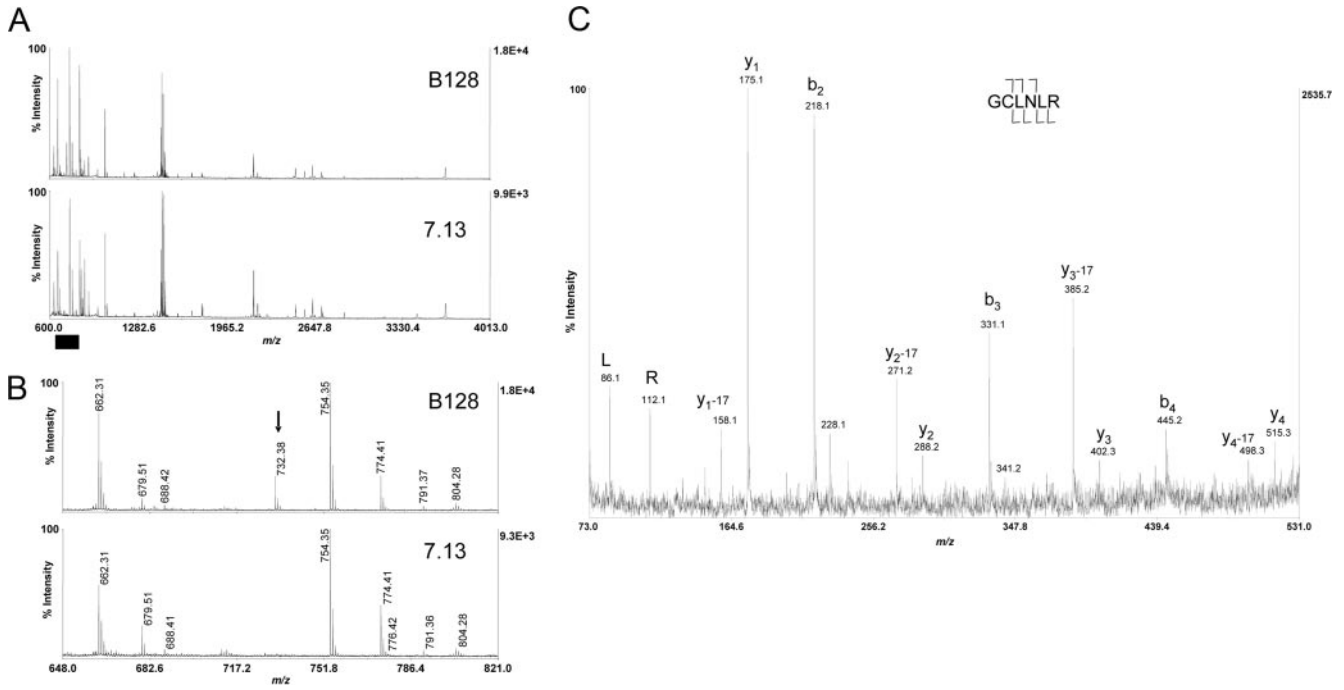

FIG. 4. **Mass spectral evidence for C296R missense mutation in strain 7.13.** *A*, MALDI-TOF peptide mass maps from trypsin digestion of FlaA from strain B128 (*upper panel*) and 7.13 (*lower panel*) that were resolved on separate gels as described under "Experimental Procedures." Approximately 75% of the FlaA sequence predicted from strain J99 present in the Swiss-Prot database (FLAA_HELPJ) was accounted for in this analysis. *B*, the mass range *m/z* 648–821 (*x axis*; denoted by the *black bar* in *A*) is expanded to highlight the presence of the B128-specific peptide at *m/z* 732.38 (*black arrow*). *C*, MALDI-TOF/TOF fragmentation spectrum of *m/z* 732.38, which is consistent with the expected fragmentation pattern for the peptide containing the C296R mutation. Labeled b-ions and y-ions are denoted by cleavage *brackets above* and *below* the sequence, respectively. The cysteine was carbamidomethylated (mass shift of +57 Da) as described under "Experimental Procedures."

investigate the roles of several additional loci of pathogenic interest identified in the DIGE/MS analysis in CagA translocation and β-catenin activation. These loci included *HP0743* (up-regulated in strain 7.13), which is predicted to encode a rod shape-determining protein; *HP0391* and *HP1286* (each up-regulated in strain B128), which are predicted to encode proteins that regulate chemotaxis or that possess hypothetical functions, respectively; and *HP0310*, an *N*-acetylglucosamine deacetylase (45, 46). These loci were selected based upon differences in bacterial morphology that we observed between strains B128 and 7.13 (Fig. 5*C*), our interest to determine whether certain microbial proteins may exert suppressive roles in *H. pylori*-induced cancer, and recent data indicating that HP0310 may function to modulate the murein layer of *H. pylori* by deacetylating peptidoglycan, a substrate that is translocated into host cells by the *cag* secretion system and induces Nod1-dependent proinflammatory responses (47). Loss of *HP0310* resulted in significantly higher levels of CagA translocation compared with levels induced by the wild-type *H. pylori* strain 7.13 (Fig. 6*B*) but did not significantly alter β-catenin activation (Fig. 6, *C* and *D*). These findings are not completely unexpected because CagA-dependent activation of β-catenin is mediated by non-phosphorylated CagA (23), and additional *H. pylori* constituents have recently been shown to regulate β-catenin activation (48). In contrast, both phenotypes were unaffected by null mutations in *HP0391*, *HP0743*, or *HP1286* (Fig. 6, *B* and *C*). These results suggest that HP0310 alters levels of peptidoglycan, thereby affecting the composition of substrates translocated by the *cag* secretion system, and indicate that multiple *H. pylori* disease-associated constituents can alter CagA translocation.

Our global survey by DIGE/MS also revealed several other differentially abundant proteins of interest. These include a member of the *H. pylori* thioredoxin system, TrxB (Table I). The membrane fraction of 7.13 contained 3.63-fold more TrxB than did the membrane fraction of B128 ($p = 0.023$), whereas the cytoplasmic levels of TrxB in strain 7.13 were 1.66-fold lower than in B128 ($p = 0.005$). Other notable proteins differentially abundant between strains B128 and 7.13 include AtpA and NapA (Table I). Compared with B128, membrane fractions from strain 7.13 expressed significantly more AtpA (1.65-fold increase; $p = 0.019$), a protein homologous to the ATP synthase unit F1 subunit, that plays a key role in the synthesis of ATP (49). NapA, a neutrophil-activating protein, was present at significantly lower levels in strain 7.13 *versus* B128 (1.3-fold lower in 7.13 cytoplasm; $p = 0.009$). Thus, DIGE/MS identified several additional candidate loci that can be targeted in future studies.

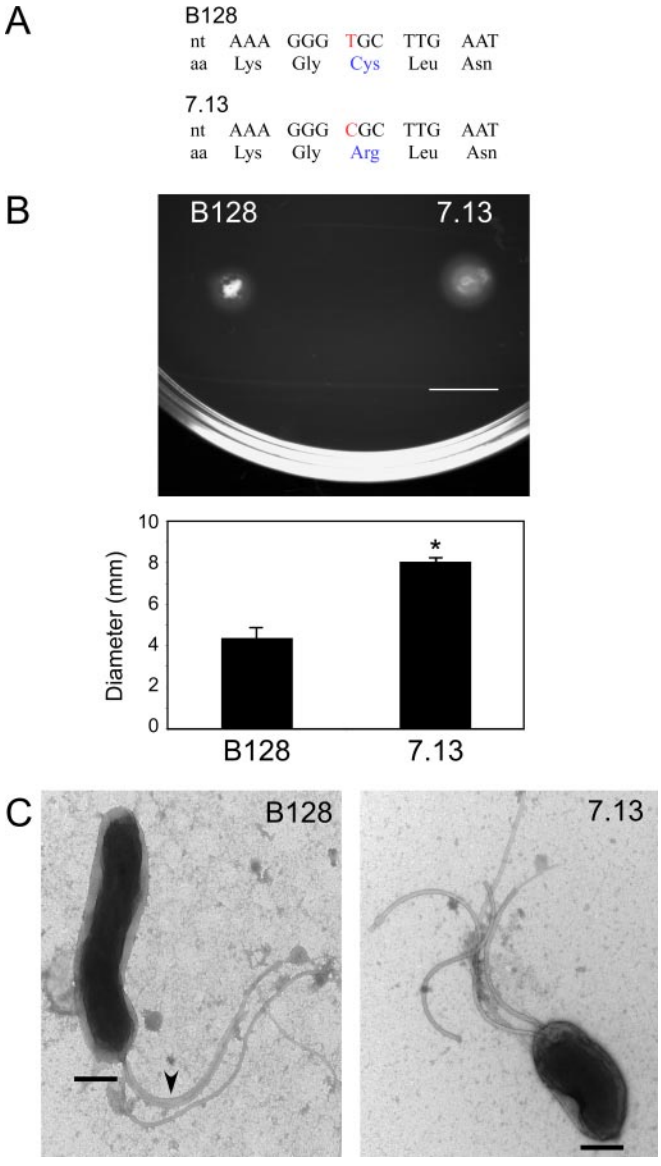

FIG. 5. **FlaA of strain 7.13 differs from FlaA of B128 in protein sequence and morphology, and strains exhibit differences in motility.** *A*, a single nucleotide change in FlaA results in a cysteine to arginine substitution in strain 7.13. *nt*, nucleotide; *aa*, amino acid. *B*, *H. pylori* strain 7.13 migrates farther in soft agar compared with strain B128. Representative images are shown of strain 7.13 and B128 growth on soft agar that is indicative of motility. Quantitative analysis of four independent motility assays is shown *below* the image. *Error bars*, S.E. *, $p < 0.05$ *versus* strain B128. *C*, differences in bacterial morphology between *H. pylori* strains B128 and 7.13 were assessed by transmission electron microscopy. *Bar*, 500 nm. *Magnification*, 25,000×. *Arrows* indicate regions where flagella are adherent to each other.

DISCUSSION

H. pylori isolates obtained from different individuals exhibit substantial genetic diversity (11–15) consistent with extensive recombination and a panmictic population structure. Differences among strains include point mutations in highly conserved genes, the presence of nonconserved and/or mosaic forms of genes, and chromosomal organization (11–15). Because of this remarkable genetic diversity, identification of *H. pylori* factors associated with virulence has been difficult; this prompted our focus on two genetically related prototype strains that differ in carcinogenic potential. By performing 2D DIGE of both cytoplasmic and membrane extracts from four independent experiments across a series of gels with an internal standard, we were able to determine statistical significance for the abundance differences identified, and PCA indicated ~5% variance between the non-carcinogenic strain B128 and the carcinogenic strain 7.13 (Fig. 2*B*). Unsupervised hierarchical clustering analysis confirmed reproducibility between replicates with minimal technical variation, further underscoring the utility of this method for the analysis of closely related samples. Our results comparing these two prototype strains identified a limited number of differentially represented proteins that we can test in future functional assays using an easily transformable carcinogenic *H. pylori* strain (7.13) and a susceptible host (Mongolian gerbils). These findings must ultimately be extended into larger populations of *H. pylori* strains that have been isolated from persons with or without gastric cancer to rigorously confirm the importance of candidate loci identified by our DIGE/MS analysis in the carcinogenic process. However, our current results have provided a foundation for these future corroborative studies, which will bring important new insights into mechanisms that mediate *H. pylori*-induced gastric carcinogenesis.

One of the most important differences detected was expression of *H. pylori* strain-specific FlaA isoforms. This analysis demonstrated that FlaA expressed by strain B128 possessed a cysteine at residue 296, whereas an arginine is normally specified at this position in strain 7.13 as well as other strains. Consistent with an arginine present at this position in the carcinogenic strain, the overall pI change for the four major FlaA isoforms is shifted to the right (more basic) in strain 7.13 as expected (Fig. 3*B*), and DNA sequencing confirmed the strain-specific presence of cysteine or arginine as expected. It is important to note in this regard that this missense mutation may have been overlooked if the complementary peptide-based ESI-LC/MS/MS ("shotgun") proteomics analysis was used unless alterations in FlaA were specifically targeted and searched. Further analysis into phenotypic differences related to this substitution revealed variations in flagellar adhesive properties in conjunction with morphological differences (Fig. 5*C*), which are consistent with the disparity in motility observed between these two strains (Fig. 5*B*). Complementation of *flaA* from strain 7.13 into the isogenic *flaA*$^-$ mutant B128 strain restored motility *in vitro*; however, this did not restore the ability of the isogenic *flaA*$^-$ mutant to colonize gerbils for which there are several potential explanations.

One possibility is that *H. pylori* flagellin exerts other functions *in vivo* in addition to regulating motility. For example,

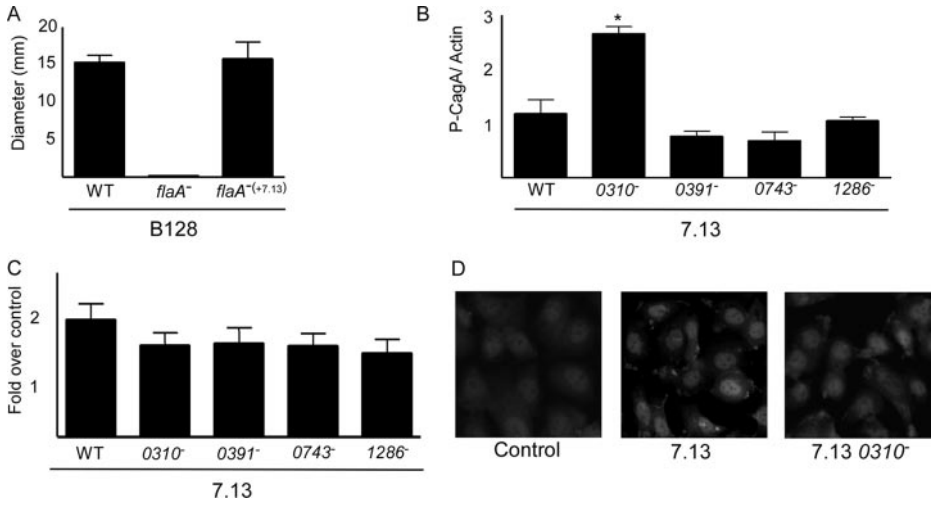

FIG. 6. **Role of candidate virulence loci identified by DIGE/MS in motility, CagA translocation, and β-catenin activation.** *A*, re-expression of *flaA* from strain 7.13 in a *flaA*$^-$ isogenic B128 mutant strain restores motility. Quantitative analysis of four independent motility assays is shown for wild-type (*WT*) strain B128, an isogenic *flaA* mutant B128 strain, and the complemented *flaA*$^-$ mutant B128 strain that re-expresses *flaA* from strain 7.13. *B*, lysates from AGS cells co-cultured with *H. pylori* wild-type strain 7.13 or the isogenic 7.13 *HP0310*$^-$, *HP0391*$^-$, *HP0743*$^-$, or *HP1286*$^-$ mutant strains were used for Western blot analysis using anti-phosphotyrosine or anti-actin antibodies. Densitometric analysis of multiple Western blot repetitions performed on at least three occasions is shown. *Error bars*, S.D. *, $p < 0.05$ *versus* wild-type strain 7.13. *C*, AGS cells were transfected with luciferase reporter constructs containing LEF/TCF binding motifs (Topflash) in the absence or presence of wild-type strain 7.13 or the isogenic 7.13 *HP0310*$^-$, *HP0391*$^-$, *HP0743*$^-$, or *HP1286*$^-$ mutant strains. Luciferase activity was determined following 24 h of treatment. *D*, AGS human gastric epithelial cells incubated with medium alone, wild-type strain 7.13, or the 7.13 *HP0310*$^-$ mutant for 6 h were immunostained with an anti-β-catenin antibody and visualized by fluorescence microscopy. Representative images are shown.

Reeves *et al.* (50) recently reported that inactivation of *flaA* significantly reduced binding of *H. pylori* to trefoil factor 1 (TFF1), a cysteine-rich protein found within gastric mucus. In that study, disruption of *flaA* also altered the production of *H. pylori* LPS as wild-type *H. pylori* was able to express both rough- and smooth-type LPS, but inactivation of *flaA* abolished the ability to express rough-type LPS (50). Flagella from mucosal Gram-negative pathogens such as *Salmonella* can induce other phenotypes, such as production of proinflammatory cytokines (51). Thus, it is possible that complementation of FlaA from strain 7.13 into strain B128 may have only partially restored functions attributable to *H. pylori* flagellin.

Unlike most prokaryotes, *H. pylori* lacks the requisite enzymes to generate glutathione and other thiol reductants. However, this pathogen does possess a thioredoxin system, including TrxB, that catalyzes the reduction of specific proteins by NADPH (52), which is critical for survival of *H. pylori* in an environment containing DNA-damaging agents (53). Infection with *H. pylori* strain 7.13 induces a severe inflammatory response in gerbils (22) that is associated with increased levels of reactive oxygen and nitrogen radicals at sites juxtaposed to colonizing organisms. Proteomics analysis demonstrated that the membrane, but not the cytoplasm, of strain 7.13 contained higher levels of TrxB than did the corresponding fractions in strain B128. Increased expression of TrxB and altered localization of thioredoxin to the membrane *versus* the cytoplasm places this defense molecule in an optimal position to scavenge extracellular oxygen and nitrogen radicals, potentially protecting strain 7.13 from lethal mutagenesis and enhancing its survival within inflamed mucosa. The neutrophil-activating protein NapA was also differentially abundant in strain B128 *versus* 7.13. Because NapA plays an important role in recruiting human neutrophils and monocytes to sites of infection (54), down-regulation of this protein may facilitate immune evasion, thus conferring a selective advantage to strain 7.13 for inducing pathogenic responses.

Another candidate virulence protein, HP0310, was identified to be present at higher levels in both the membrane and cytosolic fractions of strain 7.13 *versus* strain B128. Upon detailed inspection, however, these differences were found to result from the presence of different charged isoforms rather than an abundance change between the two strains. This difference was confirmed by genomic sequencing of *HP0310* in both B128 and 7.13 that demonstrated a single point mutation that converted a cysteine at amino acid position 34 in strain B128 to an arginine in strain 7.13. The protein encoded by the *HP0310* gene is homologous to polysaccharide deacetylase, an enzyme that catalyzes the hydrolysis of *N*-linked acetyl groups from *N*-acetylglucosamine residues or *O*-linked acetyl groups from *O*-acetylxylose residues (46). This enzyme also functions to deacetylate *N*-acetylglucosamine residues in *H. pylori* peptidoglycan (45), a substrate for the *cag* secretion system. Our current results indicate that loss of HP0310 augments CagA translocation, which may play a role in pathogenesis. Of interest, HP0310 was abundant in both cytoplasmic and membrane fractions of strain

7.13, suggesting that this protein may function not only to modify bacterial proteins and residues such as peptidoglycan prior to translocation into host cells but also to modify surface proteins present on the surfaces of neighboring epithelial cells.

In conclusion, *H. pylori* has evolved numerous strategies to facilitate its persistence within the human stomach, and one consequence of long term colonization is an increased risk of gastric cancer. By utilizing proteomics technology to contrast two closely related *H. pylori* strains that induce distinct phenotypes in animal models, we identified a focused group of proteins that may mediate carcinogenesis. By linking structure to function, we identified differences in flagellar morphology and bacterial motility that may be related to sequence differences observed in the FlaA protein. Our data also indicate that multiple classes of proteins are differentially abundant in carcinogenic strain 7.13 and its parental derivative B128, including proteins involved in responses to oxidative stress, evasion of the immune system, bacterial replication, and modification of secreted virulence constituents. These studies provide an important foundation for the investigation of the role of bacterial virulence factors in *H. pylori*-induced carcinogenesis on a deeper level. Such results would ultimately permit physicians to more appropriately focus diagnostic and eradication strategies on high risk populations to optimize prevention of subsequent neoplastic events.

* This work was supported, in whole or in part, by National Institutes of Health Grants CA116087, DK58587, and CA77955 (to R. M. P.) and DK058404 (to The Vanderbilt Digestive Diseases Research Center). This work was also supported by the Vanderbilt Academic Venture Capital Fund.

S The on-line version of this article (available at http://www.mcponline.org) contains supplemental material.

‡‡ To whom correspondence should be addressed: Division of Gastroenterology, Vanderbilt University School of Medicine, 1030C MRB IV, 2215B Garland Ave., Nashville, TN 37232-2279; Tel.: 615-322-5200; Fax: 615-343-6229; E-mail: richard.peek@vanderbilt.edu.

REFERENCES

1. Peek, R. M., Jr., and Crabtree, J. E. (2006) Helicobacter infection and gastric neoplasia. *J. Pathol.* **208,** 233–248
2. Moss, S. F., and Sood, S. (2003) *Helicobacter pylori*. *Curr. Opin. Infect. Dis.* **16,** 445–451
3. Peek, R. M., Jr., and Blaser, M. J. (2002) Helicobacter pylori and gastrointestinal tract adenocarcinomas. *Nat. Rev. Cancer* **2,** 28–37
4. Uemura, N., Okamoto, S., Yamamoto, S., Matsumura, N., Yamaguchi, S., Yamakido, M., Taniyama, K., Sasaki, N., and Schlemper, R. J. (2001) Helicobacter pylori infection and the development of gastric cancer. *N. Engl. J. Med.* **345,** 784–789
5. Parsonnet, J., Friedman, G. D., Vandersteen, D. P., Chang, Y., Vogelman, J. H., Orentreich, N., and Sibley, R. K. (1991) Helicobacter pylori infection and the risk of gastric carcinoma. *N. Engl. J. Med.* **325,** 1127–1131
6. Nomura, A., Stemmermann, G. N., Chyou, P. H., Kato, I., Perez-Perez, G. I., and Blaser, M. J. (1991) Helicobacter pylori infection and gastric carcinoma among Japanese Americans in Hawaii. *N. Engl. J. Med.* **325,** 1132–1136
7. Forman, D. (1996) Helicobacter pylori and gastric cancer. *Scand. J. Gastroenterol. Suppl.* **220,** 23–26
8. Correa, P. (1996) Helicobacter pylori and gastric cancer: state of the art. *Cancer Epidemiol. Biomarkers Prev.* **5,** 477–481
9. Wong, B. C., Lam, S. K., Wong, W. M., Chen, J. S., Zheng, T. T., Feng, R. E., Lai, K. C., Hu, W. H., Yuen, S. T., Leung, S. Y., Fong, D. Y., Ho, J., Ching, C. K., and Chen, J. S. (2004) Helicobacter pylori eradication to prevent gastric cancer in a high-risk region of China: a randomized controlled trial. *JAMA* **291,** 187–194
10. Ernst, P. B., Peura, D. A., and Crowe, S. E. (2006) The translation of *Helicobacter pylori* basic research to patient care. *Gastroenterology* **130,** 188–206, quiz 212–213
11. Falush, D., Stephens, M., and Pritchard, J. K. (2003) Inference of population structure using multilocus genotype data: linked loci and correlated allele frequencies. *Genetics* **164,** 1567–1587
12. Salama, N., Guillemin, K., McDaniel, T. K., Sherlock, G., Tompkins, L., and Falkow, S. (2000) A whole-genome microarray reveals genetic diversity among *Helicobacter pylori* strains. *Proc. Natl. Acad. Sci. U.S.A.* **97,** 14668–14673
13. Go, M. F., Kapur, V., Graham, D. Y., and Musser, J. M. (1996) Population genetic analysis of *Helicobacter pylori* by multilocus enzyme electrophoresis: extensive allelic diversity and recombinational population structure. *J. Bacteriol.* **178,** 3934–3938
14. Alm, R. A., Ling, L. S., Moir, D. T., King, B. L., Brown, E. D., Doig, P. C., Smith, D. R., Noonan, B., Guild, B. C., deJonge, B. L., Carmel, G., Tummino, P. J., Caruso, A., Uria-Nickelsen, M., Mills, D. M., Ives, C., Gibson, R., Merberg, D., Mills, S. D., Jiang, Q., Taylor, D. E., Vovis, G. F., and Trust, T. J. (1999) Genomic-sequence comparison of two unrelated isolates of the human gastric pathogen *Helicobacter pylori*. *Nature* **397,** 176–180
15. Tomb, J. F., White, O., Kerlavage, A. R., Clayton, R. A., Sutton, G. G., Fleischmann, R. D., Ketchum, K. A., Klenk, H. P., Gill, S., Dougherty, B. A., Nelson, K., Quackenbush, J., Zhou, L., Kirkness, E. F., Peterson, S., Loftus, B., Richardson, D., Dodson, R., Khalak, H. G., Glodek, A., McKenney, K., Fitzegerald, L. M., Lee, N., Adams, M. D., Hickey, E. K., Berg, D. E., Gocayne, J. D., Utterback, T. R., Peterson, J. D., Kelley, J. M., Cotton, M. D., Weidman, J. M., Fujii, C., Bowman, C., Watthey, L., Wallin, E., Hayes, W. S., Borodovsky, M., Karp, P. D., Smith, H. O., Fraser, C. M., and Venter, J. C. (1997) The complete genome sequence of the gastric pathogen *Helicobacter pylori*. *Nature* **388,** 539–547
16. Salama, N. R., Gonzalez-Valencia, G., Deatherage, B., Aviles-Jimenez, F., Atherton, J. C., Graham, D. Y., and Torres, J. (2007) Genetic analysis of *Helicobacter pylori* strain populations colonizing the stomach at different times postinfection. *J. Bacteriol.* **189,** 3834–3845
17. Israel, D. A., Salama, N., Krishna, U., Rieger, U. M., Atherton, J. C., Falkow, S., and Peek, R. M., Jr. (2001) Helicobacter pylori genetic diversity within the gastric niche of a single human host. *Proc. Natl. Acad. Sci. U.S.A.* **98,** 14625–14630
18. Backert, S., Ziska, E., Brinkmann, V., Zimny-Arndt, U., Fauconnier, A., Jungblut, P. R., Naumann, M., and Meyer, T. F. (2000) Translocation of the *Helicobacter pylori* CagA protein in gastric epithelial cells by a type IV secretion apparatus. *Cell. Microbiol.* **2,** 155–164
19. Odenbreit, S., Püls, J., Sedlmaier, B., Gerland, E., Fischer, W., and Haas, R. (2000) Translocation of *Helicobacter pylori* CagA into gastric epithelial cells by type IV secretion. *Science* **287,** 1497–1500
20. Higashi, H., Tsutsumi, R., Muto, S., Sugiyama, T., Azuma, T., Asaka, M., and Hatakeyama, M. (2002) SHP-2 tyrosine phosphatase as an intracellular target of *Helicobacter pylori* CagA protein. *Science* **295,** 683–686
21. Tammer, I., Brandt, S., Hartig, R., König, W., and Backert, S. (2007) Activation of Abl by *Helicobacter pylori*: a novel kinase for CagA and crucial mediator of host cell scattering. *Gastroenterology* **132,** 1309–1319
22. Franco, A. T., Israel, D. A., Washington, M. K., Krishna, U., Fox, J. G., Rogers, A. B., Neish, A. S., Collier-Hyams, L., Perez-Perez, G. I., Hatakeyama, M., Whitehead, R., Gaus, K., O'Brien, D. P., Romero-Gallo, J., and Peek, R. M., Jr. (2005) Activation of beta-catenin by carcinogenic *Helicobacter pylori*. *Proc. Natl. Acad. Sci. U.S.A.* **102,** 10646–10651
23. Murata-Kamiya, N., Kurashima, Y., Teishikata, Y., Yamahashi, Y., Saito, Y., Higashi, H., Aburatani, H., Akiyama, T., Peek, R. M., Jr., Azuma, T., and Hatakeyama, M. (2007) Helicobacter pylori CagA interacts with E-cadherin and deregulates the beta-catenin signal that promotes intestinal transdifferentiation in gastric epithelial cells. *Oncogene* **26,** 4617–4626
24. Amieva, M. R., Vogelmann, R., Covacci, A., Tompkins, L. S., Nelson, W. J., and Falkow, S. (2003) Disruption of the epithelial apical-junctional complex by *Helicobacter pylori* CagA. *Science* **300,** 1430–1434
25. Suzuki, M., Mimuro, H., Suzuki, T., Park, M., Yamamoto, T., and Sasakawa,

C. (2005) Interaction of CagA with Crk plays an important role in *Helicobacter pylori*-induced loss of gastric epithelial cell adhesion. *J. Exp. Med.* **202,** 1235–1247
26. Bagnoli, F., Buti, L., Tompkins, L., Covacci, A., and Amieva, M. R. (2005) Helicobacter pylori CagA induces a transition from polarized to invasive phenotypes in MDCK cells. *Proc. Natl. Acad. Sci. U.S.A.* **102,** 16339–16344
27. Atherton, J. C., Cao, P., Peek, R. M., Jr., Tummuru, M. K., Blaser, M. J., and Cover, T. L. (1995) Mosaicism in vacuolating cytotoxin alleles of *Helicobacter pylori*: association of specific *vacA* types with cytotoxin production and peptic ulceration. *J. Biol. Chem.* **270,** 17771–17777
28. Cover, T. L., Krishna, U. S., Israel, D. A., and Peek, R. M., Jr. (2003) Induction of gastric epithelial cell apoptosis by *Helicobacter pylori* vacuolating cytotoxin. *Cancer Res.* **63,** 951–957
29. Hessey, S. J., Spencer, J., Wyatt, J. I., Sobala, G., Rathbone, B. J., Axon, A. T., and Dixon, M. F. (1990) Bacterial adhesion and disease activity in *Helicobacter* associated chronic gastritis. *Gut* **31,** 134–138
30. Gerhard, M., Lehn, N., Neumayer, N., Borén, T., Rad, R., Schepp, W., Miehlke, S., Classen, M., and Prinz, C. (1999) Clinical relevance of the *Helicobacter pylori* gene for blood-group antigen-binding adhesin. *Proc. Natl. Acad. Sci. U.S.A.* **96,** 12778–12783
31. Prinz, C., Schöniger, M., Rad, R., Becker, I., Keiditsch, E., Wagenpfeil, S., Classen, M., Rösch, T., Schepp, W., and Gerhard, M. (2001) Key importance of the *Helicobacter pylori* adherence factor blood group antigen binding adhesin during chronic gastric inflammation. *Cancer Res.* **61,** 1903–1909
32. Tonge, R., Shaw, J., Middleton, B., Rowlinson, R., Rayner, S., Young, J., Pognan, F., Hawkins, E., Currie, I., and Davison, M. (2001) Validation and development of fluorescence two-dimensional differential gel electrophoresis proteomics technology. *Proteomics* **1,** 377–396
33. Lilley, K. S., and Friedman, D. B. (2006) Difference gel electrophoresis DIGE. *Drug Discov. Today Technol.* **3,** 347–353
34. Alban, A., David, S. O., Bjorkesten, L., Andersson, C., Sloge, E., Lewis, S., and Currie, I. (2003) A novel experimental design for comparative two-dimensional gel analysis: two-dimensional difference gel electrophoresis incorporating a pooled internal standard. *Proteomics* **3,** 36–44
35. Friedman, D. B., Hill, S., Keller, J. W., Merchant, N. B., Levy, S. E., Coffey, R. J., and Caprioli, R. M. (2004) Proteome analysis of human colon cancer by two-dimensional difference gel electrophoresis and mass spectrometry. *Proteomics* **4,** 793–811
36. Lilley, K. S., and Friedman, D. B. (2004) All about DIGE: quantification technology for differential-display 2D-gel proteomics. *Expert Rev. Proteomics* **1,** 401–409
37. Friedman, D. B., Stauff, D. L., Pishchany, G., Whitwell, C. W., Torres, V. J., and Skaar, E. P. (2006) Staphylococcus aureus redirects central metabolism to increase iron availability. *PLoS Pathog.* **2,** e87
38. Backert, S., Kwok, T., Schmid, M., Selbach, M., Moese, S., Peek, R. M., Jr., König, W., Meyer, T. F., and Jungblut, P. R. (2005) Subproteomes of soluble and structure-bound *Helicobacter pylori* proteins analyzed by two-dimensional gel electrophoresis and mass spectrometry. *Proteomics* **5,** 1331–1345
39. Wessel, D., and Flügge, U. I. (1984) A method for the quantitative recovery of protein in dilute solution in the presence of detergents and lipids. *Anal. Biochem.* **138,** 141–143
40. Israel, D. A., Salama, N., Arnold, C. N., Moss, S. F., Ando, T., Wirth, H. P., Tham, K. T., Camorlinga, M., Blaser, M. J., Falkow, S., and Peek, R. M., Jr. (2001) Helicobacter pylori strain-specific differences in genetic content, identified by microarray, influence host inflammatory responses. *J. Clin. Investig.* **107,** 611–620
41. Backert, S., Moese, S., Selbach, M., Brinkmann, V., and Meyer, T. F. (2001) Phosphorylation of tyrosine 972 of the *Helicobacter pylori* CagA protein is essential for induction of a scattering phenotype in gastric epithelial cells. *Mol. Microbiol.* **42,** 631–644
42. Kim, J. S., Chang, J. H., Chung, S. I., and Yum, J. S. (1999) Molecular cloning and characterization of the *Helicobacter pylori fliD* gene, an essential factor in flagellar structure and motility. *J. Bacteriol.* **181,** 6969–6976
43. Suerbaum, S., Josenhans, C., and Labigne, A. (1993) Cloning and genetic characterization of the *Helicobacter pylori* and *Helicobacter mustelae flaB* flagellin genes and construction of *H. pylori flaA*- and *flaB*-negative mutants by electroporation-mediated allelic exchange. *J. Bacteriol.* **175,** 3278–3288
44. Eaton, K. A., Suerbaum, S., Josenhans, C., and Krakowka, S. (1996) Colonization of gnotobiotic piglets by *Helicobacter pylori* deficient in two flagellin genes. *Infect. Immun.* **64,** 2445–2448
45. Wang, G., Olczak, A., Forsberg, L. S., and Maier, R. J. (2009) An oxidative stress-induced peptidoglycan deacetylase in *Helicobacter pylori. J. Biol. Chem.* **284,** 6790–6800
46. Psylinakis, E., Boneca, I. G., Mavromatis, K., Deli, A., Hayhurst, E., Foster, S. J., Vårum, K. M., and Bouriotis, V. (2005) Peptidoglycan N-acetylglucosamine deacetylases from *Bacillus cereus*, highly conserved proteins in *Bacillus anthracis. J. Biol. Chem.* **280,** 30856–30863
47. Viala, J., Chaput, C., Boneca, I. G., Cardona, A., Girardin, S. E., Moran, A. P., Athman, R., Mémet, S., Huerre, M. R., Coyle, A. J., DiStefano, P. S., Sansonetti, P. J., Labigne, A., Bertin, J., Philpott, D. J., and Ferrero, R. L. (2004) Nod1 responds to peptidoglycan delivered by the *Helicobacter pylori cag* pathogenicity island. *Nat. Immunol.* **5,** 1166–1174
48. Franco, A. T., Johnston, E., Krishna, U., Yamaoka, Y., Israel, D. A., Nagy, T. A., Wroblewski, L. E., Piazuelo, M. B., Correa, P., and Peek, R. M., Jr. (2008) Regulation of gastric carcinogenesis by *Helicobacter pylori* virulence factors. *Cancer Res.* **68,** 379–387
49. Owen, R. J., and Xerry, J. (2003) Tracing clonality of *Helicobacter pylori* infecting family members from analysis of DNA sequences of three housekeeping genes (*ureI*, *atpA* and *ahpC*), deduced amino acid sequences, and pathogenicity-associated markers (*cagA* and *vacA*). *J Med. Microbiol.* **52,** 515–524
50. Reeves, E. P., Ali, T., Leonard, P., Hearty, S., O'Kennedy, R., May, F. E., Westley, B. R., Josenhans, C., Rust, M., Suerbaum, S., Smith, A., Drumm, B., and Clyne, M. (2008) Helicobacter pylori lipopolysaccharide interacts with TFF1 in a pH-dependent manner. *Gastroenterology* **135,** 2043–2054, 2054.e1–2
51. Gewirtz, A. T., Simon, P. O., Jr., Schmitt, C. K., Taylor, L. J., Hagedorn, C. H., O'Brien, A. D., Neish, A. S., and Madara, J. L. (2001) Salmonella typhimurium translocates flagellin across intestinal epithelia, inducing a proinflammatory response. *J. Clin. Investig.* **107,** 99–109
52. Holmgren, A. (1985) Thioredoxin. *Annu. Rev. Biochem.* **54,** 237–271
53. Ritz, D., Lim, J., Reynolds, C. M., Poole, L. B., and Beckwith, J. (2001) Conversion of a peroxiredoxin into a disulfide reductase by a triplet repeat expansion. *Science* **294,** 158–160
54. Evans, D. J., Jr., Evans, D. G., Takemura, T., Nakano, H., Lampert, H. C., Graham, D. Y., Granger, D. N., and Kvietys, P. R. (1995) Characterization of a *Helicobacter pylori* neutrophil-activating protein. *Infect. Immun.* **63,** 2213–2220